Assessing the contribution of odor-active compounds in icewine considering odor mixture-induced interactions through gas chromatography–olfactometry and Olfactoscan

Yue Ma, Noëlle Béno, Ke Tang, Yuanyi Li, Marie Simon, Yan Xu, Thierry Thomas-Danguin

▶ **To cite this version:**

Yue Ma, Noëlle Béno, Ke Tang, Yuanyi Li, Marie Simon, et al.. Assessing the contribution of odor-active compounds in icewine considering odor mixture-induced interactions through gas chromatography–olfactometry and Olfactoscan. Food Chemistry, 2022, 388, pp.132991. 10.1016/j.foodchem.2022.132991 . hal-03713076

HAL Id: hal-03713076
https://hal.inrae.fr/hal-03713076v1

Submitted on 22 Jul 2024

HAL is a multi-disciplinary open access archive for the deposit and dissemination of scientific research documents, whether they are published or not. The documents may come from teaching and research institutions in France or abroad, or from public or private research centers.

L'archive ouverte pluridisciplinaire **HAL**, est destinée au dépôt et à la diffusion de documents scientifiques de niveau recherche, publiés ou non, émanant des établissements d'enseignement et de recherche français ou étrangers, des laboratoires publics ou privés.

Distributed under a Creative Commons Attribution - NonCommercial 4.0 International License

Version of Record: https://www.sciencedirect.com/science/article/pii/S0308814622009530
Manuscript_690e45c1a67bde38bf34fad219d281af

Title: Assessing the contribution of odor-active compounds in icewine considering odor mixture-induced interactions through gas chromatography–olfactometry and Olfactoscan

Authors: Yue MA [a, b, c], Noëlle BÉNO [c], Ke TANG [a,b], Yuanyi LI [a,b], Marie SIMON [c], Yan XU [a,b]*, Thierry THOMAS-DANGUIN [c]*

[a] Lab of Brewing Microbiology and Applied Enzymology, School of Biotechnology, Jiangnan University, 1800 Lihu Avenue, Wuxi, Jiangsu 214122, P. R. China

[b] Key Laboratory of Industrial Biotechnology of Ministry of Education, State Key Laboratory of Food Science and Technology, Jiangnan University, 1800 Lihu Avenue, Wuxi, Jiangsu 214122, People's Republic of China.

[c] Centre des Sciences du Goût et de l'Alimentation, INRAE, CNRS, Institut Agro Dijon, Université Bourgogne Franche-Comté, Dijon, France.

* To whom correspondence should be addressed.

(Tel: +86 510 85918197; Fax: +86 510 85918201) E-mail: yxu@jiangnan.edu.cn;

(Tel: +33 380 693084; Fax: +33 380 693227) E-mail: thierry.thomas-danguin@inrae.fr;

E-mail addresses of the co-authors:

Yue MA: 7160201007@vip.jiangnan.edu.cn

Noëlle BÉNO: noelle.beno@inrae.fr

Ke TANG: tandy81@jiangnan.edu.cn

Yuanyi LI: 876791762@qq.com

Marie SIMON: marie.simon@inrae.fr

© 2022 published by Elsevier. This manuscript is made available under the CC BY NC user license
https://creativecommons.org/licenses/by-nc/4.0/

22 **Abstract**

23 The sensory impact of odor-active compounds on icewine aroma could be influenced by perceptual
24 interactions with other odor-active compounds. The aim of this study was to establish an approach
25 to evaluate the contribution of odor-active compounds found in icewine considering
26 mixture-induced perceptual interactions. By comparing the impact of key odorants detected in
27 icewine following a gas chromatography–olfactometry approach with an Olfactoscan-based
28 methodology using a background odor of icewine, 69 odor zones were detected, and their related
29 compounds were further identified. The results revealed that icewine background odor could exert
30 odor masking or enhancement on key odorants when they are considered in the complex wine
31 aroma buffer. Several compounds can induce qualitative changes in the overall wine aroma. This
32 study underlined the efficiency of Olfactoscan-like approaches to screen for the real impact of key
33 odorants and to pinpoint specific compounds that could be highly influential once embedded in the
34 aroma buffer.

35 **Keywords:** key odorants, Olfactometer, background odor, aroma buffer, perceptual interactions

36

1. Introduction

Wine flavor is built mostly on the perception of the numerous odor-active compounds found in the wine matrix (Polášková, Herszage, & Ebeler, 2008). These odor-active compounds can be screened from a huge body of wine volatiles by gas chromatography–olfactometry (GC–O; Dunkel et al., 2014) and further identified using a variety of separation and spectroscopic techniques, such as comprehensive two-dimensional gas chromatography combined with time-of-flight mass spectrometry (GC × GC–TOFMS; Lyu, Ma, Xu, Nie, & Tang, 2019). The sensory impact of odor-active compounds can be evaluated by different GC–O procedures (De-La-Fuente-Blanco & Ferreira, 2020), such as Aroma Extract Dilution Analysis (AEDA; Schieberle, 1995) and Detection Frequency analysis (DF; Pollien et al., 1997). Although these GC–O procedures are pivotal to reveal the most intense odor-active compounds when isolated, their actual sensory impact could be influenced not only by interactions with nonvolatile compounds of the wine matrix (Sáenz-Navajas et al., 2010) but also perceptual interactions induced by the olfactory processing of the mixture of odor-active compounds (Thomas-Danguin et al., 2014).

Perceptual interactions between odorants have been observed in wines and other alcoholic beverages. Esters have been shown to play a crucial role in berry fruit odor notes (Escudero, Campo, Fariña, Cacho, & Ferreira, 2007) but also to mask or enhance fruity and floral notes at various levels in model wine recombination (Lytra, Tempere, Le Floch, de Revel, & Barbe, 2013), and to induce synergistic effects on the overall aroma perception of Chinese cherry wines (Niu et al., 2019). Synergistic effects induced by aldehydes such as benzaldehyde, furfural, and vanillin were observed in a *Huangjiu* aroma reconstitution (Yu et al., 2020). Individual γ-lactones were unlikely to be key aroma compounds, but combinations of some γ-lactones might act additively or synergistically to contribute to the ‘apricot’ aroma of white wine (Siebert et al., 2018). Ethylphenols had a masking

effect on wine fruity notes even at subliminal concentrations (Tempere et al., 2016). Monoterpenes such as linalool were found to influence the fruity aroma of Pinot Gris wine (Tomasino, Song, & Fuentes, 2020). Furthermore, the complex mixture of the most common wine odor-active compounds, such as ethyl esters, fusel alcohols, volatile phenols, have been suggested to be able to exert an aroma-buffering effect that had both the ability to make unnoticeable the omission of one of its components or the addition of many single odorants, particularly those with fruity characteristics (Ferreira, 2010).

Because of the critical impact of perceptual interactions on wine aroma perception, the actual contribution of odor-active compounds should be systematically checked by reconstitution, addition, or omission procedures (Grosch, 2001). Nevertheless, the compounds tested in these procedures have usually been selected based on GC−O results that tend to highlight only those single compounds at a concentration above the detection threshold, thus preventing the contribution of subthreshold compounds or other mixture-induced perceptual effects (Atanasova et al., 2005; Thomas-Danguin et al., 2014). New methods, such as the Olfactoscan (Burseg & de Jong, 2009; Thomsen et al., 2017), OASIS (Hattori, Takagaki, & Fujimori, 2003), InnOscent (Villiere, Le Roy, Fillonneau, & Prost, 2018), and Gas Chromatography-Pedestal Olfactometry (GC–PO) (Williams, Sartre, Parisot, Kurtz, & Acree, 2009), have been developed to overcome this deficiency. The InnOscent system is based on a chromatographic device, whose configuration allows for omission or recombination experiments through the connection of recovery disposals to the outlets for fraction collection. The OASIS, GC–PO, and Olfactoscan systems use an external device to deliver more or less adjustable background odors that combine with compounds eluted from a GC–O device at the sniffing port. These technologies can achieve online complex odor-active compounds recombination. The differences in these technologies are mainly determined by the external device

that produces the background odor. In Olfactoscan, the external equipment to provide the background odor is a multichannel dynamic dilution olfactometer that allows the shaping of the odor background in terms of composition (mixture) and intensity (dilution). Thus, it is possible to apply the Olfactoscan technique to evaluate the contribution of each candidate key aroma compound of a food or beverage within a well-controlled and adjustable aroma buffer.

Icewine is a rare, intensely sweet wine made from grapes naturally frozen on the vine at temperatures below or equal to –7 °C. The icewine grape undergoes a special dehydration process and freeze–thaw cycles, and its must for icewine making, which is pressed from frozen grapes, is a concentrated grape juice with more sugars, acids, and other dissolved solids, resulting in slower-than-normal fermentation. These different winemaking procedures lead to a unique aroma characteristic of icewine (Ma, Xu, & Tang, 2021). The typical aroma of icewine has been described as honey, tropical fruit, apricot, caramel, raisin, nutty and floral (Ma, Xu, & Tang, 2021), and more than 80 odor-active compounds were detected by GC–O from different grape varieties (Lan et al., 2019; Ma, Tang, Xu, & Li, 2017). The contribution of these odorants was evaluated by comparing the dilution factors (FDs) obtained from AEDA and odor activity value (OAV), which is the ratio between the odorant concentration in a sample and its detection threshold. Although the contribution of the most impactful compounds has been verified by recombination studies in icewine mixtures (Lan et al., 2019; Ma et al., 2017), the differences still remaining between aroma reconstruction based on identified key odorants and the original wine suggested that the contribution of some compounds, which could benefit from mixture perceptual interactions, might have been overlooked.

The aim of this study was to establish a method based on the Olfactoscan technique to evaluate the contribution of odor-active compounds in icewine considering complex odorant

mixture-induced effects. We especially compared the impact of odorants detected in icewine using a classical GC–O approach (i.e. without background odor) with those identified following the Olfactoscan analysis using the icewine odor as the background odor. The results should help reconsider the key status of several odor-active compounds and reveal new compounds, initially considered minor, on the global odor profile of icewine.

2. Materials and methods

2.1 Samples

Commercial icewine was purchased from ChangYu Winery (Yantai, Shandong Province, China). This icewine was made from Vidal grapes harvested in 2019 from the Huanren region (Liaoning Province, China), and its quality meets the standards of the Vintners Quality Alliance system. This icewine was chosen because the Huanren region dominates the major production of icewine in China, and it was selected by wine experts to ensure it was typical of the wine styles in this region. All samples were stored horizontally at 11 °C in the dark before use.

2.2 Chemicals

Absolute ethanol (≥99.8%, GC grade), dichloromethane (≥99.8%, GC grade), and methanol (≥99.9%, GC grade) were purchased from Sigma-Aldrich (St. Louis, MO, USA). Ultrapure water was obtained from a Milli-Q purification system (Millipore, Bedford, MA, USA). Analytical-grade anhydrous sodium sulfate was purchased from Sigma-Aldrich (St. Louis, MO, USA). Aroma reference compounds (purity > 95%), which were used as standards for odor-active compounds identification, were purchased from Sigma-Aldrich (St. Louis, MO, USA).

2.3 Aroma extraction methods

Solid-phase extraction (SPE) was used to extract volatile compounds following a procedure modified from the one we conducted previously (Ma et al., 2017). Briefly, the extraction tube

(LiChrolut ® EN, Merck; 500 mg of phase) was first rinsed with 10 mL of dichloromethane, then 10 mL of methanol and 10 mL of a water–ethanol mixture (11%, ethanol by volume). Then, 100 mL of sample was filtered through the tube at a flow rate of 1 mL/min. Then, the column was rinsed with 20 mL of ultrapure water to remove sugars, pigment, or other low-molecular-weight polar compounds, and then the column was dried under vacuum before eluting the sorbent. To obtain the icewine aroma extract, 10 mL of dichloromethane were used to elute organic compounds from the extraction tube, and anhydrous sodium sulfate was added to the eluate to remove trace water. Finally, a nitrogen stream was used to concentrate the eluate to a final volume of 0.25 mL for GC–O or Olfactoscan analysis.

2.4 Gas chromatography–Olfactometry (GC–O) and Olfactoscan analysis conditions

GC–O and Olfactoscan analyses were conducted on an Agilent 7890B GC (Agilent Technologies, Santa Clara, CA, USA) coupled to a flame ionization detector (FID) and an olfactory detection port (ODP). In comparison with GC–O, Olfactoscan provided a constant background odor and combined this background odor with odors eluted from the gas chromatograph at the outlet of a GC–O system (Figure 1). Both analyses used a dynamic dilution olfactometer (OM4/b; Burghart, Wedel, Germany), in which the outlet was connected to the ODP of the GC by a homemade T-piece to provide a stable airflow (Barba, Beno, Guichard, & Thomas-Danguin, 2018; Burseg & de Jong, 2009). For each GC–O and Olfactoscan analysis (Figure 1), 1 µL of icewine aroma extract was injected into the split/splitless inlet of the GC (splitless mode, purge flow to split vent 25 mL/min at 0.5 min). The GC system was equipped with a 30 m × 0.25 mm i.d. fused silica capillary column coated with a 0.5-µm layer of polyethylene glycol (DB-Wax; Agilent Technologies); helium was used as a carrier gas at a constant flow rate of 2 mL/min. The column effluent split to the FID and ODP was 1:1. The injector and transfer line temperatures were set at 250 °C. The olfactory port was

heated at 240 °C to prevent the condensation of high boiling point compounds. The oven temperature was held at 50 °C for 2 min, increased to 240 °C at 6 °C/min, and then held at 240 °C for 10 min. Following the GC–O configuration, the olfactometer delivered to the ODP a constant flow of nitrogen (155 mL/min), stabilized at a temperature of 20 °C. In that case, one of the olfactometer chambers, kept at 20°C, was filled with 40 mL of pure water to ensure a constant humidity level of the gas stream. Following the Olfactoscan configuration, the olfactometer delivered the same total constant flow of nitrogen to the ODP (155 mL/min), which produced a stable icewine odor background. To generate the icewine odor, one of the olfactometer chambers, kept at 20 °C, was filled with icewine. The icewine in the olfactometer chamber was continuously renewed with a peristaltic pump (Gilson, Middleton, USA) at 1 mL/min to keep the icewine background odor intensity and quality stable. Nitrogen went through the chambers at a constant flow rate fixed at 155 mL/min, in the icewine chamber only, to generate the icewine odor at high level (OLFH) and at a constant flow of 78 mL/min in the icewine chamber, combined with a constant flow of 77mL/min in the water chamber to produce the icewine background odor at the low level (OLFL); the total flow still being 155 mL/min. The different flow rates were computer-controlled and checked before each sniffing session using an external flowmeter. The quantitative and qualitative chemical stability of the background odor was checked before the beginning of the experiment, with two replications. The quantitative stability was evaluated by monitoring the total volatile content of the wine background odor using a photoionization detector ppbRAE 3000 (RAE, Lyon, France). The results showed that the total volatile content decreased by less than 5% during a 90-min period of monitoring, while the GC run lasted less than 45 min. The qualitative stability was evaluated by comparing the chromatograms of two odor samples, which were collected from the outlet of GC–O at the beginning and at the end of the GC run. The results

showed that there was no significant change in the volatile compound profile (chromatogram) between the two sampling times.

2.5 Subjects

Nineteen healthy subjects (24 to 65 years old) were recruited from the INRAE center and participated in the GC–O/Olfactoscan analyses. These subjects first went through two screening tests to evaluate: (i) their performance in detecting and identifying different odor qualities using the European Test of Olfactory Capabilities (ETOC, Thomas-Danguin et al., 2003), and (ii) their ability to maintain selective attention with time using the Bourdon Test (Bourdon T.I.B. test, Swets & Zeitlinger BV, Calisse, The Netherlands). Before the actual acquisition sessions, they were also asked to perform one sniffing training session to become familiarized with the GC–O procedure and devices. In this familiarization session, 1 µL of a solution of eight odorants diluted in dichloromethane (Supplementary Table 1) was injected into the GC inlet. Participants were requested not to smoke or eat for 1 h before the session and received one gift for each session.

2.6 Gas chromatography–Olfactometry and Olfactoscan analysis

We conducted three sessions in the formal test. In the first session, we applied traditional gas chromatography–olfactometry (GC–O) analysis to evaluate the contribution of each candidate key aroma compound. In the other two sessions, we applied the Olfactoscan technique to evaluate the contribution of each candidate key aroma compound within the aroma buffer of icewine at high (OLFH) and low level (OLFL). These two levels were determined based on odor intensity as evaluated by 3 experienced internal subjects from the laboratory staff, who tested these levels to ensure that they corresponded to distinct low-to-moderate, and moderate-to-high, but still comfortable, odor intensities. The Detection Frequency (DF) method was selected as the GC–O and Olfactoscan measurement procedure. During each sniffing, subjects were asked to detect the

198 presence of an odor by pushing a button rapidly as soon as they perceived it and trying to give a
199 descriptor that was as accurate as possible of the perceived odor. The responses were recorded by a
200 Gerstel Olfactory Detection Port Recorder system (Gerstel GmbH & Co., Mülheim, Germany), and
201 audio tracks were recorded *via* a microphone simultaneously with the response recordings. The
202 duration of each sniffing was 35 min, starting after solvent elution. By comparing the results
203 obtained through GC–O analysis and Olfactoscan, the contribution of each compound to the global
204 odor profile of icewine can be evaluated considering odor mixture-induced effects in icewine.

205 **2.7 Data process for detection frequency (DF) method**

206 The data obtained in GC–O and Olfactoscan were processed using the DF method (Pollien et al.,
207 1997) to perform an overall grouping of all the responses given by all the subjects into Odor Zones
208 (OZs) on the basis of their retention time closeness. Because of the background odor in Olfactoscan,
209 it was more difficult to determine OZs; thus, a semiautomatic method was established to define and
210 standardize the OZs between GC–O and Olfactoscan. The GC–O result of the odor cocktail solution
211 (Supplementary Table 1) in the training session and the GC–O result of the icewine extract were
212 used to optimize different parameters of the semiautomatic method to obtain the OZs as precisely as
213 possible. In this semiautomatic method, retention time was first transferred to Kovats retention
214 indices (RIs) by means of *n*-alkane injections (C8–C32), and then the detection frequency was
215 calculated from the number of odor events that occurred in a range of 5 RI values. This integration
216 process was applied because of the variability of subject response times. Then, the detection
217 frequency as a function of the RI was analyzed by *R* software (version 4.0.1) using the *findPeak*
218 function of the *quantmod* package (Ryan et al., 2020) to determine detection frequency peaks. In
219 this procedure, a noise level of 3 for frequency was chosen as a threshold to consider a significant
220 peak corresponding to an OZ. The obtained OZs were further manually checked in the raw data to

221 evaluate whether any important OZs were missing or duplicated considering the odor descriptors
222 given by the subjects. Finally, OZs from GC–O and Olfactoscan analysis were defined, and each
223 OZ was characterized by: 1) its nasal impact frequency (NIF, %), which corresponded to the
224 proportion of detection by the panelists of each OZ (number of subjects who detected / total number
225 of subjects) c; 2) its odor descriptors given by subjects; and 3) the first, last and average retention
226 indices of the response given by the subjects.

227 **2.8 Identification of the impact compounds**

228 The compounds responsible for OZs were identified by: 1) GC–MS (Ma et al., 2017) and
229 comparing the RI and odor descriptor of a candidate compound with the RI and odor descriptor of
230 its pure standards under the same GC conditions as GC–O; 2) comparing the odor descriptor of a
231 candidate compound with its odor descriptor reported in the database; 3) comparing the
232 experimental RI of a candidate compound with its RI reported in the National Institute of Standards
233 and Technology (NIST) mass spectral library and 4) comprehensive two-dimensional gas
234 chromatography and time-of-flight mass spectrometry (GC × GC–TOFMS) analysis.

235 GC × GC–TOFMS analysis was performed on a LECO Pegasus 4D® GC × GC–TOFMS
236 instrument (LECO Corporation, St. Joseph, MI, USA), basically consisting of an Agilent GC model
237 7890B, LECO dual nozzle thermal modulator system, and secondary column thermostat connected
238 to a time-of-flight mass spectrometer. A polar column DB-FFAP (60 m × 0.25 mm × 0.25 μm,
239 Agilent Technologies, Santa Clara, CA, USA) was used as the first-dimension (1st D) column, and a
240 medium polarity column Rxi-17Sil MS (1.5 m × 0.25 mm ×0.25 μm; Restek, Bellefonte, PA, USA)
241 was used as the second-dimension (2nd D) column. After optimizing several GC × GC parameters by
242 raising the rate of column temperature and modulation period, the following GC × GC conditions
243 were used. Split injection (1.0 μL) was applied, and the split ratio was set as 5:1. The initial

temperature of the primary oven was held at 40 °C for 1 min, programmed at 10 °C/min to 85 °C for 1 min and then raised at 4 °C/min to 135 °C for 1 min, then at 3 °C/min to 210 °C for 1 min, and finally programmed at 8 °C/min to 240 °C for 15 min. The secondary oven temperature was 5 °C higher than the primary oven during the chromatographic run. The modulator temperature was offset +15 °C from the primary oven, and the modulation time was set at 3 s (0.5 s hot, 1.0 s cold pulses). Helium (99.999%) was used as the carrier gas at a constant flow of 1.0 mL/min. The temperatures of the GC injector and the transfer line were set to 240 °C. The ion source was programmed at 230 °C and EI voltage at 70 eV. An electron multiplier at 1400 V, a mass range of *m/z* 30−400, and an acquisition frequency of 100 spectra/s were programmed. LECO ChromaTOF® Workstation (version 4.44) was used for acquisition control and data processing. Automated peak detection and spectral deconvolution were employed. The baseline signal was drawn just above the noise and the segmented signal-to-noise (S/N) for peak picking was set at 200:1 for a minimum of 2 apexing masses. Within individual chromatograms, subpeaks in the 2nd dimension were required to meet a S/N ≥6 and a minimum spectral similarity match of 650 (65%) to be combined. The reference peak was determined by the unique mass ion and the overall purity and shape of the peak. All chromatograms were compared spectrally with the reference peak chromatogram from the NIST Mass Spectral Library and Wiley Registry™ of Mass Spectral Data Library. The mass spectra of a reference peak with similarity scores greater than 700 were selected as candidate peaks, and its name was assigned to the automated peak detection result. Kovats retention indices (RIs) of peaks were calculated by injection of a reference solution of *n*-alkanes under the same GC × GC conditions (C8−C29). The RI of each peak was compared with its RI reported in the NIST library, and peaks with RI differences exceeding 20 units were excluded from the peak identification.

2.9 Data analysis

Statistical analyses were performed with *R* software (version 4.0.1). Principal component analysis (PCA) was carried out on the nasal impact frequency (NIF, %) of every odor descriptor for the high impact odor peaks over the icewine background odor level by using the *prcomp* function of the *tempR* package (Castura, 2016). The PCAs were used to provide a global representation of the trajectory of impact odor peaks in relation to the evolution of odor descriptors based on the first and second principal components. The categorized odor descriptors trajectories in each impact odor peak are illustrated by connecting three different icewine background odor levels. The icewine background odor levels were none for GC–O analysis, low level for Olfactoscan analysis (OLFL) and high level for Olfactoscan analysis (OLFH).

3. Results and discussion

3.1 Odor zone defined in GC–O and Olfactoscan analysis by the detection frequency (DF) method

A total of 2430 odor events were recorded from 19 subjects during all the analysis methods. These events were distributed as follows: GC–O analysis (GCO, 820), Olfactoscan analysis at a low background odor level (OLFL, 870), and Olfactoscan analysis at a high background odor level (OLFH, 740). The raw detection frequency data are reported in Figure 2a for each analysis method. A first observation is that the number of odor events in the OLFH method is lower than in other methods, suggesting a mixture-induced masking effect of the icewine background odor on the detection of odorants. A semiautomatic method was applied to define the odor zones (OZs) in each analysis condition. First, an automatic peak detection function led to the identification of 75 OZs in GCO, 65 OZs in OLFL, and 56 OZs in OLFH. The frequency of the highest peaks for these OZs is illustrated in Figure 2b based on the average RI. The OZs identified following automatic detection were then manually checked to ensure that no important OZs were missing or that duplicated OZs

were mistakenly considered. This manual check was conducted for two main reasons. First, there can be coelution of odorants in a narrow RI range so that two different odor events generated by the same subject can be grouped into a single OZ. In that case, the OZs were separated or pooled based on the events' RI and odor descriptors. For example, the OZ with an RI range from 1470 to 1500 was manually separated into two OZs (1470–1485 and 1485–1500). Second, there can be an intense odor that might be lasting for a long time so that more than one odor event would be generated by the same subject. Thus, the OZs that had close RIs (± 10) and were described with the same odor descriptor were combined into a single OZ. For example, the two OZs (1345–1355 and 1355–1365) were combined into one OZ (1345–1365). The RI range (± 10) was selected based on the GC–O analysis of the odor cocktail solution performed in the training session (Supplementary Table 1), which showed that for an intense odor, the RI range can be from 15 to 30. A threshold frequency above or equal to 4, corresponding to a proportion of 20%, was used to remove noise from the results. In previous reports (Barba et al., 2018; Machiels, Istasse, & van Ruth, 2004), various threshold values from 12.5% to 40% were selected as the noise level. In the absence of any clear recommendations and based on the GC–O result of the odor cocktail solution performed in the training session, a threshold of 4 was chosen to avoid excluding too many OZs. After manual checking, a total of 69 OZs were considered from all the analysis methods and distributed as follows: GC–O (66), OLFL (65), and OLFH (60). The final OZ data are represented in Figure 2c based on average RIs and reported in Table 1.

3.2 Peak identification and odor-active compound contribution in GC–O and Olfactoscan analysis

To identify the odor-active compounds responsible for each OZ obtained in GC–O and Olfactoscan analysis, GC–MS and GC × GC–TOFMS analyses were conducted. The identification

313 of several compounds was further checked through injection in GC–MS of pure standards under the
314 same GC conditions as in GC–O (marked by 'S' in Table 2). Finally, 57 OZs were associated with
315 63 compounds identified by GC–MS and GC × GC–TOFMS analysis; there was coelution for 4
316 OZs. These results were confirmed by injection of pure standards under the same GC conditions
317 (Ma et al., 2017). The OZs that failed to be related to the compounds identified by GC × GC–
318 TOFMS analysis were defined by at least two of the following methods: 1) comparing the RI and
319 odor descriptor of a candidate compound with the RI and odor descriptor of its pure standards under
320 the same GC conditions; 2) comparing the odor descriptor of a candidate compound with its odor
321 descriptor reported in *The Good Scents Company* database; and 3) comparing the experimental RI
322 of a candidate compound with the RI reported in the NIST Mass Spectral Library. The OZ
323 identification results are given in Table 2. Due to different GC conditions in the GC–MS and
324 GC × GC–TOFMS analyses, the RI of several compounds calculated from the detection response
325 obtained in the GC-MS analysis was different from the RI calculated from the GC × GC–TOFMS
326 analysis. To highlight these compounds with different RI but double-checked with the injection of
327 standard compounds, we tagged them with a '*' in Table 2.

328 Detection frequency (DF) or nasal impact frequency (NIF, %) was used to evaluate the
329 contribution of OZs identified in icewine by GC–O analysis without background odor (GCO) or
330 Olfactoscan analysis with background odor (OLFH, OLFL). Although the NIF value is not a direct
331 measurement of the perceived odor intensities, it increases with intensity and concentration (Pollien
332 et al., 1997). Therefore, the NIF can be used to compare peak intensities between different
333 compounds. Based on GC–O results of the odor cocktail solution performed in the training session,
334 the compounds with DF ≥ 12 or NIF > 60% were considered as high impact compounds; they are
335 marked in purple in Figure 2c.

There were 12 OZs, 10 OZs, and 11 OZs considered to have a high impact in the GCO, OLFH, and OLFL analyses, respectively. Among these OZs, 7 OZs were in common in the three analyses. The compounds associated with these peaks were 3-methyl-1-butanol (peak 12), 3-methylbutanoic acid (peak 39), 2-acetyl-1-pyrroline (peak 18), 2-methylbutanoic acid (peak 36), acetophenone (peak 36), methional (peak 27), 1-octen-3-one (peak 17) and guaiacol (peak 48). For peak 36, there might be two compounds for the OZ since they were eluted at very close RI based on the GC × GC–TOFMS result. Among other high odor impact compounds, 2-ethyl-3,5-dimethylpyrazine (peak 25) was identified in GCO and OLFL analyses with the same NIF (63.2%), but it was detected in OLFH analysis with a lower value (NIF = 57.9%). Ethyl isobutyrate (peak 1, NIF = 73.7%), geraniol (peak 46, NIF = 68.4%), *β*-damascenone (peak 46, NIF = 68.4%), 3-mercapto-1-hexanol (peak 46, NIF = 68.4%), eugenol (peak 59, NIF = 63.2%) and ethyl butyrate (peak 4, NIF = 63.2%) were only identified as high impact compounds in GC–O. Interestingly, most of these compounds had fruity or sweet-like odors that would likely be masked by the wine background odor in OLF analyses. For peak 46, there might be three compounds for the OZ since they were eluted at very close RI based on the GC × GC–TOFMS result (see Table 2). The high-impact odorants found only in OLFH (phenylethyl alcohol, 2-methyl-1-propanol, 1-hexanol) and OLFL (hotrienol, nerol oxide, (*Z*)-3-hexen-1-ol) were also detected in GC–O analysis, but at lower NIF values (from 47.4% to 57.9%).

3.3 Mixture-induced effect of icewine background odor on the detection and identification of odor-active compounds

The mixture-induced effect of icewine background odor on the detection of odor-active compounds was evaluated by comparing the NIF value between GC–O analysis (without icewine background odor) and Olfactoscan analysis (with icewine background odor at high, OLFH, and low

359 levels, OLFL). Since a threshold value (20%) was applied to consider significant NIF in the
360 identification of OZs, the same threshold (DF = 4) was applied to consider a significant NIF
361 difference between GC–O and Olfactoscan. If an OZ's NIF in Olfactoscan was significantly lower
362 than the NIF in GC–O, the icewine background odor induced a masking effect for this OZ.
363 Conversely, if an OZ's NIF in Olfactoscan was significantly higher than the NIF in GC–O, the
364 icewine background odor induced an enhancement of the perception of this OZ, likely due to
365 additive, synergy, or blending effects (for a review of these mixture effects see, e.g.,
366 Thomas-Danguin et al., 2014).
367 The results showed that with a high level of icewine background odor (OLFH), the NIF value of
368 18 OZs decreased significantly (from –21.1% to –57.9%), which indicated that these OZs were
369 masked by the icewine odor. The NIF of 4 OZs increased significantly (from +21.1% to +42.1%),
370 which indicated an enhancement effect of the icewine odor on these OZs. The contrast between
371 OLFH and GCO data is illustrated in Figure 3a, thus highlighting the influence of the icewine odor
372 on each OZ. The compounds associated with the most importantly masked OZs were ethyl
373 isobutyrate (peak 1, NIF decrease in OLFH –57.9%), ethyl isovalerate (peak 6, –42.1%), ethyl
374 butyrate (peak 4, –36.8%), isoeugenol (peak 67, –36.8%), 3-methyl-1-butanol (peak 12, –31.6%),
375 eugenol (peak 59, –31.6%), 2-acetylthiazole (peak 37, –31.6%), benzeneacetaldehyde (peak 35, –
376 31.6%), γ-undecalactone (peak 63, –31.6%) and isobutyl acetate (peak 3, –31.6%). The compounds
377 associated with OZs that benefited from enhancement with the icewine odor were methional (peak
378 27, +21.1%), diethyl succinate (peak 38, +21.1%), and phenol (peak 52, +21.1%). Moreover, peak
379 66 was considered nonsignificant in GCO since its NIF value was 10.5%, but in OLFH, its NIF was
380 52.6%. Three compounds, namely, 9-decenoic acid, geranic acid, and isophytol, might be related to
381 this peak based on GC × GC–TOFMS analysis, RIs, and odor descriptors.

382 At a low level of icewine background odor (OLFL), a masking effect occurred for 11 OZs, with a
383 decrease in NIF values compared to GC–O in the range of 21.1% to 57.9%. Enhancement occurred
384 for 6 OZs with an increase in NIF of 21.1% to 26.3% (Figure 3b). The compounds associated with
385 the OZs that were masked in OLFL were ethyl isobutyrate (peak 1, –57.9%), ethyl butyrate (peak 4,
386 –47.4%), ethyl isovalerate (peak 6, –36.8%), 3-methyl-1-butanol (peak 12, –31.6%), geraniol (peak
387 46, –-31.6%), *β*-damascenone (peak 46, –31.6%) and 3-mercapto-1-hexanol (peak 46, –31.6%). The
388 compounds associated with OZs in enhancement with the icewine odor were guaiacol (peak 48,
389 +26.3%), 1-heptanol (peak 26, +26.3%), *γ*-heptalactone (peak 44, +26.3%), ethyl pyruvate (peak 15,
390 +21.1%) and methional (peak 27, +21.1%). Peak 13 was also found to benefit from enhancement
391 (+26.3%), and 2 odorants (2-pentylfuran and 2-hexanol) might contribute on the basis of GC × GC–
392 TOFMS analysis, RIs, and odor descriptors.
393 We observed that 8 OZs were masked at both icewine background odor levels (peaks 1, 3, 4, 6,
394 12, 35, 59, 63; red color in Figure 3c) and that 1 OZ was enhanced at both levels (methional, peak
395 27); 39 OZs were not influenced by the background odor regardless of the level (black color in
396 Figure 3c). Nevertheless, the results also showed that the mixture-induced effects caused by the
397 icewine background odor were level-dependent (Figure 3d). Indeed, between OLFH and OLFL, as
398 the concentration of icewine background odor mixture decreased, the DF of 10 OZs increased,
399 while the DF of 6 OZs decreased. In OLFH, 10 OZs were masked only at high concentration (peaks
400 5, 14, 22, 37, 42, 53, 54, 64, 67, 68, purple color in Figure 3c); 2 OZs were enhanced only at high
401 concentration (peaks 38, 52; light blue color in Figure 3c); 3 OZs were masked at low concentration
402 (peaks 18, 46, 55; rose color in Figure 3c); and 5 OZs were enhanced at low concentration (peaks
403 13, 15, 26, 44, 48; light green color in Figure 3c). We did not observe any OZ that was masked at

404 one concentration but enhanced at the other concentration. This comparison between GC–O and
405 Olfactoscan is visualized in Figure 3c and Figure 3d.
406 In addition to mixture-induced intensity effects such as masking and enhancement, the
407 Olfactoscan approach provides cues about the modification of odor quality of odor-active
408 compounds once embedded in the icewine odor. To investigate these odor quality modifications, the
409 descriptors provided by the subjects during GC–O and Olfactoscan runs were categorized into 10
410 categories based on an adapted version of the wine aroma wheel (Supplementary Figure 1) proposed
411 by Noble (Noble et al., 1987). The categories are as follows: caramelized, chemical, earthy, floral,
412 fruity, microbiological, nutty, spicy, vegetative, and woody. Two categories of the original wine
413 aroma wheel (pungent and oxidized) were not considered relevant for icewine. When no descriptor
414 was provided by subjects for an odor event, a category "not identified" was used, and when the OZ
415 was not detected, it was categorized as "not detected". Individual responses within GCO, OLFH,
416 and OLFL analyses were dispatched in the 10 categories and expressed as percentages. Principal
417 component analysis (PCA) was conducted to follow odor quality modification induced by the
418 background odor for the high impact OZ (NIF> 60%). The first 2 dimensions of PCA accounted for
419 34% of the total variance, which increased to 55.7% when the first 4 dimensions were considered.
420 The PCA maps are presented in Figure 4 as trajectories of odor quality evolution as a function of the
421 odor background level. The starting point was the GC–O analysis, i.e., with no background odor of
422 icewine, then was the low level of icewine odor (OLFL), and finally was the high level of
423 background odor (OLFH).
424 As a first observation, peak 7 (2-methyl-1-propanol), peak 17 (1-octen-3-one), peak 19
425 (1-hexanol), peak 28 (nerol oxide), peak 36 (2-methylbutanoic acid, acetophenone), and peak 39
426 (3-methylbutanoic acid) did not move widely on the first 2 planes of the PCA, meaning that the

427 odor of these compounds was not very affected by the icewine background odor and that their
428 characteristic odor was still highly recognizable even with a high level background icewine odor.
429 The same conclusion can be suggested for peak 18 (2-acetyl-1-pyrroline), peak 25
430 (2-ethyl-3,5-dimethylpyrazine) and peak 49 (phenylethyl alcohol) since their trajectories are least in
431 the first PCA plot. The trajectories for peak 1 (ethyl isobutyrate), peak 4 (ethyl butyrate), peak 12
432 (3-methyl-1-butanol) and peak 59 (eugenol) obviously changed from right to left in Figure 4a,
433 which confirmed the masking of the odor of these compounds by increasing levels of the
434 background odor as previously observed. Therefore, it is likely that the odor of these compounds
435 blended with the aromatic buffer of the icewine odor that contained relatively high concentrations
436 of ethanol, ethyl esters, fusel alcohols, and volatile phenols (Escudero et al., 2004). Interestingly, for
437 3-methyl-1-butanol (peak 12), not only did the increasing levels of icewine odor mask the
438 perception of its characteristic odor, but it seems that its odor quality also changed from floral-sweet
439 to fruity. Conversely, the trajectories of peak 48 (guaiacol) and peak 27 (methional) changed from
440 left to right in Figure 4a, in line with the previously observed enhanced effect for these peaks. For
441 peak 27, the vegetative odor of methional seemed to be maintained in the icewine aroma buffer,
442 while the woody odor of guaiacol likely changed to a more floral or caramelized odor. For peak 21
443 ((*Z*)-3-hexen-1-ol) and peak 34 (hotrienol), as the background icewine odor level increased, their
444 descriptors changed to a fruity aspect.

445 **3.4 General discussion**

446 Odor-active compounds in Vidal icewine have been previously identified through the AEDA
447 approach followed by recombination and omission tests (Ma et al., 2017). In the present study,
448 based on the same wine (but different vintage) using the same extraction method, we chose the DF
449 approach, which was the only method that can be efficient for the Olfactoscan condition. Indeed,

450 due to the odor background in this condition, a threshold-based method could not be selected, and a
451 method relying on odor intensity rating would have been too cognitively demanding for the
452 panelists and likely weakly sensitive. In previous research, it was suggested that the results obtained
453 by DF readily reflected odor intensity (Pollien et al., 1997; Van Ruth, 2001), and this method could
454 be more rapid and more repeatable than AEDA (Delahunty, Eyres, & Dufour, 2006), while results of
455 both methods were found highly correlated (Le Guen, Prost, & Demaimay, 2000). Comparing the
456 odor-active compounds identified by DF with those previously obtained by AEDA (Ma et al., 2017),
457 we found that 76% of the compounds with a flavor dilution factor above or equal to 9 in AEDA
458 were well detected by DF, with NIF values above or equal to 47.4%, and 21% of odor-active
459 compounds with NIFs from 21.1% to 36.8%. Only one compound, ethyl acetate, was not detected
460 by DF, which can be explained by the fact that this compound was eluted before the solvent and
461 thus not delivered at the olfactory port. Indeed, the whole gas flow at the sniffing port was sucked
462 back by the olfactometer until the end of the solvent peak to prevent panelists from inhaling
463 dichloromethane. Compared to AEDA, the DF method allowed detection of more OZs, and some of
464 these OZs showed a high contribution, such as peak 1 (ethyl isobutyrate, NIF = 73.7%), peak 18
465 (2-acetyl-1-pyrroline, NIF = 89.5%), peak 25 (2-ethyl-3,5-dimethylpyrazine, NIF = 63.2%), peak
466 36 (2-methylbutanoic acid/acetophenone, NIF = 78.9%), peak 39 (3-methylbutanoic acid, NIF =
467 94.7%) and peak 59 (eugenol, NIF = 63.2%). The identification of these compounds might be due
468 to the difference in the samples between the two studies (same icewine but different vintages) or to
469 the limited number of subjects involved in the AEDA (2 to 4; (Ma et al., 2017). Indeed, the
470 sensitivity, discrimination ability, risk of inattention, and specific anosmia of the sniffers could
471 result in missed peaks (Pollien et al., 1997). Another difference between AEDA and DF concerned
472 peak 46. In AEDA, the flavor dilution factor of this peak was the highest, as large as 2187; however,

473 in the DF method, its NIF was not the highest, only 68.4%. This difference might be explained by
474 subjects' sensitivity, since the AEDA method is based on detection thresholds, and/or by
475 suprathreshold sensitivity as reflected by Steven's power function slope, which can be low, meaning
476 that the increase of odor intensity as a function of concentration is small. Notably, *β*-damascenone
477 was identified as a putative odor-active compound responsible for peak 46. This compound has both
478 a very low detection threshold (0.002 µg/l in water; Buttery, Teranishi, Flath, & Ling, 1989) and a
479 low Steven's power function slope (Ferreira, 2010). Nevertheless, GC × GC–TOFMS analysis
480 indicated that geraniol and 3-mercapto-1-hexanol were also candidate odorants for peak 46 since
481 they were eluted at very similar RI.
482 As a major result, the present study showed that although odor-active compounds can be considered
483 to have a significant aroma contribution when they are separated, their perception can be influenced
484 by a mixture-induced effect (Ferreira, 2012; Ma, Tang, Xu, & Thomas-Danguin, 2021;
485 Thomas-Danguin et al., 2014) , so that their odor contribution might be very different when they are
486 embedded in the complex aroma of icewine. Roughly, we observed that 57% of the odor-active
487 compounds were not highly affected by mixture effects, while 30% were masked and 13% benefited
488 from enhancement. Previous research based on binary mixture models showed that synergy, or
489 hyper-addition, is rare but may occur mostly at low-intensity levels (Ferreira, 2012). In our study,
490 we observed only a few cases of increase in the NIF for a compound when it is added to the
491 complex odor mixture formed by the icewine aroma delivered under OLF conditions; we
492 considered that such an NIF increase would be indicative of hyper- or partial-additive enhancement
493 effects. Based on our experimental protocol, we cannot affirm that a hyper-addition occurred since
494 partial addition can also explain our observations. Indeed, partial addition could have been induced
495 by the amount of the target compound actually present in the icewine background odor.

Nevertheless, our results indicated that enhancement (hyper- or partial-addition) appeared mostly in OZ, which had a relatively low NIF (≤ 31.6%), and in the OLFL condition (67% of cases), in which a low level of icewine background odor was delivered. Among the compounds for which enhancement was observed, the Olfactoscan analysis highlighted several odorants that were not considered in the GC–O analysis because their contribution was below the noise threshold. 2-Pentylfuran and/or 2-hexanol (peak 13), γ-heptalactone (peak 44), and 9-decenoic acid and/or geranic acid and/or isophytol (peak 66) benefited from enhancement and were thus only considered impact odorants under the mixture conditions. Interestingly, these compounds were not considered icewine key odorants before because they had not been detected by AEDA (Ma et al., 2017). Strikingly, only one compound (methional, peak 27) benefited from enhancement with the icewine background odor at both low and high levels. This compound was already considered a high-impact odorant in GC–O, but its impact likely increased when embedded in icewine aroma buffer. Moreover, the vegetative usually cooked potato-like odor of methional seemed to be maintained in the icewine aroma buffer. This odorant, which is related to oxidation or aging in fermented beverages (Escudero, Hernández-Orte, Cacho, & Ferreira, 2000), was found to be involved in perceptual interactions in binary mixtures (Burseg & de Jong, 2009). However, its detection probability in such simple mixtures was already proven to be strongly dependent on the compound with which it was mixed, suggesting highly intricate interactions in the case of complex mixtures. Guaiacol is another odorant that benefited from enhancement with the icewine odor, but in contrast with methional odor, we observed a shift in odor quality under OLFL conditions, suggesting that this compound interacted with the icewine odor at low intensity to contribute to a floral or caramelized character. This compound associated with the woody character of wine was found to develop perceptual interactions with the fruity component of wine (Atanasova, Thomas-Danguin,

519 Langlois, Nicklaus, & Etievant, 2004). In particular, at low background concentration level,
520 guaiacol could boost fruity character, while at higher concentration level, the woody odor could be
521 perceived at the expense of fruity odor (Atanasova et al., 2005).

522 Wine aromatic buffer has previously been reported to be able to suppress the effect of many
523 odorants added to it, particularly those with fruity characteristics (Escudero et al., 2004; Ferreira,
524 2010). Our results confirmed that several odorants carrying a fruity or floral-like odor were masked
525 once in the wine background odor. Several of these compounds had a relatively high NIF in GC–O
526 (3-methyl-1-butanol, ethyl isobutyrate, ethyl butyrate, and eugenol), meaning that they can be
527 identified as high impact odorants. However, once in the complex wine mixture, their impact would
528 be much lowered, or they may have a similar odor quality contribution to the overall fruity/floral
529 icewine odor. Such a general contribution has been proposed following the concept of aroma
530 vectors (Ferreira et al., 2016), supported, for instance, by the idea that the contribution of several
531 ethyl esters can be mimicked by only one of them (De-La-Fuente-Blanco, Sáenz-Navajas, Valentin,
532 & Ferreira, 2020). Enhancement has also been reported to be able to occur between these ethyl
533 esters (Lytra et al., 2013; Niu, Liu, & Xiao, 2020), which reinforces the idea that they contribute to
534 a general fruity character. In the case of 3-methyl-1-butanol, we found that it remained a high
535 impact odorant even in the icewine odor but that in the complex mixture, the odor quality associated
536 with its OZ changed to a more fruity-sweet character. This result is in line with previous reports
537 demonstrating that 3-methyl-1-butanol can indirectly impact wine odor quality and contribute to the
538 aromatic complexity of wine depending on its concentration, although it was shown to mask fruity
539 odor notes in model solutions. (Cameleyre, Lytra, Tempere, & Barbe, 2015).

540 Since the central aim of this study was to assess the contribution of odor-active compounds found
541 in icewine considering odor mixture-induced interactions, we have chosen to use an extraction

542 method (SPE) that provided a “total extract”. This methodological choice was made to test our
543 hypothesis that odor-active compounds, actually found in the wine but usually not considered,
544 might have been overlooked because their potential importance might only be observed in complex
545 odor mixture conditions. However, it is known that, if such extraction methods can extract up to 100%
546 of the odor-active compounds present in the original product, they do not provide a representative
547 sampling of those compounds transferred to the vapor phase at very different proportions,
548 depending on their specific volatilities and their interactions with the product matrix
549 (De-La-Fuente-Blanco & Ferreira, 2020). Therefore, it cannot be ruled out that some of the
550 compounds (e.g., polar compounds) considered in the present study might have been overestimated,
551 and further studies should investigate the sensory impact of the newly highlighted compounds in the
552 overall icewine aroma.

553 **4. Conclusions**

554 This study is among the very first attempts to evaluate the contribution of odor-active compounds
555 considering the mixture-induced effect on a complex aroma (here icewine). This study relies on the
556 Olfactoscan set-up, which allowed us to consider the impact of a single odorant on the global aroma
557 online during GC–O analysis. To analyze the data, a semiautomatic method was used to allow the
558 identification of odor zones in a similar way both in GC–O and Olfactoscan approaches based on
559 the detection frequency method. The results showed that considering a key odorant in the
560 background odor of icewine could reveal mixture-induced effects such as masking or enhancement,
561 resulting in a lower or higher detection probability of the characteristic odor of this compound or in
562 a modification of the overall wine aroma supporting qualitative perceptual interactions. In that sense,
563 the Olfactoscan approach can lead to reconsider the impact of key odorants and reveal specific
564 compounds that could be highly influential, through masking, partial-addition, or hyper-addition,

565 once embedded in the aroma buffer. Nevertheless, this study also stressed the high complexity of
566 perceptual odor interactions in real food and beverages, which advocates for the development of
567 systematic research studies to better understand the impact of a compound, or a group of
568 compounds, in complex aroma mixtures.

569 **Funding**

570 This work was supported by the National Key R&D Program (2016YFD0400504), National
571 First-class Discipline Program of Light Industry Technology and Engineering (LITE 2018–12),
572 China Scholarship Council (201806790033), and Postgraduate Research & Practice Innovation
573 Program of Jiangsu Provence (KYCX18_1788).

574 **Acknowledgments**

575 The authors are grateful to the financial support from China Scholarship Council and all the
576 subjects who participated in the sensory experiments.

577 **References**

578 Atanasova, B., Thomas-Danguin, T., Langlois, D., Nicklaus, S., Chabanet, C., & Etiévant, P. (2005).
579 Perception of wine fruity and woody notes: influence of peri-threshold odorants. *Food*
580 *Quality and Preference, 16*(6), 504-510.

581 Atanasova, B., Thomas-Danguin, T., Langlois, D., Nicklaus, S., & Etievant, P. (2004). Perceptual
582 interactions between fruity and woody notes of wine. *Flavour and Fragrance Journal, 19*(6),
583 476-482.

584 Barba, C., Beno, N., Guichard, E., & Thomas-Danguin, T. (2018). Selecting odorant compounds to
585 enhance sweet flavor perception by gas chromatography/olfactometry-associated taste
586 (GC/O-AT). *Food Chemistry, 257*, 172-181. doi:10.1016/j.foodchem.2018.02.152

587 Burseg, K., & de Jong, C. (2009). Application of the olfactoscan method to study the ability of

saturated aldehydes in masking the odor of methional. *Journal of Agricultural and Food Chemistry, 57*(19), 9086-9090.

Buttery, R. G., Teranishi, R., Flath, R. A., & Ling, L. C. (1989). Fresh tomato volatiles: composition and sensory studies. In Roy Teranishi, Ron G. Buttery, & F. Shahidi (Eds.), *Flavor Chemistry: Trends and Developments* (pp. 213-222). Washington, DC: American Chemical Society.

Cameleyre, M., Lytra, G., Tempere, S., & Barbe, J. C. (2015). Olfactory impact of higher alcohols on red wine fruity ester aroma expression in model solution. *Journal of Agricultural and Food Chemistry, 63*(44), 9777-9788. doi:10.1021/acs.jafc.5b03489

Castura, J. C. (2016). tempR: Temporal sensory data analysis. *R Package Version 0.9, 9*.

De-La-Fuente-Blanco, A., & Ferreira, V. (2020). Gas chromatography olfactometry (GC-O) for the (Semi) quantitative screening of wine aroma. *Foods, 9*(12), 1892.

De-La-Fuente-Blanco, A., Sáenz-Navajas, M. P., Valentin, D., & Ferreira, V. (2020). Fourteen ethyl esters of wine can be replaced by simpler ester vectors without compromising quality but at the expense of increasing aroma concentration. *Food Chemistry, 307*, 125553.

Delahunty, C. M., Eyres, G. T., & Dufour, J. P. (2006). Gas chromatography-olfactometry. *Journal of Separation Science, 29*(14), 2107-2125.

Dunkel, A., Steinhaus, M., Kotthoff, M., Nowak, B., Krautwurst, D., Schieberle, P., & Hofmann, T. (2014). Nature's chemical signatures in human olfaction: a foodborne perspective for future biotechnology. *Angewandte Chemie International Edition, 53*(28), 7124-7143.

Escudero, A., Campo, E., Fariña, L., Cacho, J., & Ferreira, V. (2007). Analytical characterization of the aroma of five premium red wines. Insights into the role of odor families and the concept of fruitiness of wines. *Journal of Agricultural and Food Chemistry, 55*(11), 4501-4510.

611 Escudero, A., Gogorza, B., Melus, M. A., Ortin, N., Cacho, J., & Ferreira, V. (2004).
612 Characterization of the aroma of a wine from Maccabeo. Key role played by compounds
613 with low odor activity values. *Journal of Agricultural and Food Chemistry, 52*(11),
614 3516-3524. doi:10.1021/jf0353411

615 Escudero, A., Hernández-Orte, P., Cacho, J., & Ferreira, V. (2000). Clues about the role of
616 methional as character impact odorant of some oxidized wines. *Journal of Agricultural and*
617 *Food Chemistry, 48*(9), 4268-4272.

618 Ferreira, V. (2010). Volatile aroma compounds and wine sensory attributes. In A. G. Reynolds (Ed.),
619 *Managing Wine Quality: Viticulture and Wine Quality, Vol. 1* (pp. 3-28). Cambridge, UK:
620 Woodhead Publishing.

621 Ferreira, V. (2012). Revisiting psychophysical work on the quantitative and qualitative odour
622 properties of simple odour mixtures: a flavour chemistry view. Part 1: intensity and
623 detectability. A review. *Flavour and Fragrance Journal, 27*(2), 124-140.

624 Ferreira, V., Sáenz-Navajas, M. P., Campo, E., Herrero, P., de la Fuente, A., & Fernández-Zurbano,
625 P. (2016). Sensory interactions between six common aroma vectors explain four main red
626 wine aroma nuances. *Food Chemistry, 199*, 447-456.

627 Grosch, W. (2001). Evaluation of the key odorants of foods by dilution experiments, aroma models
628 and omission. *Chemical Senses, 26*(5), 533-545.

629 Hattori, S., Takagaki, H., & Fujimori, T. (2003). Evaluation of Japanese green tea extract using
630 GC/O with original aroma simultaneously input to the sniffing port method (OASIS). *Food*
631 *Science and Technology Research, 9*(4), 350-352.

632 Lan, Y. B., Xiang, X. F., Qian, X., Wang, J. M., Ling, M. Q., Zhu, B. Q., . . . Duan, C. Q. (2019).
633 Characterization and differentiation of key odor-active compounds of 'Beibinghong' icewine

and dry wine by gas chromatography-olfactometry and aroma reconstitution. *Food Chemistry, 287*, 186-196. doi:10.1016/j.foodchem.2019.02.074

Le Guen, S., Prost, C., & Demaimay, M. (2000). Critical comparison of three olfactometric methods for the identification of the most potent odorants in cooked mussels (Mytilus edulis). *J. Agric. Food Chem., 48*(4), 1307-1314.

Lytra, G., Tempere, S., Le Floch, A., de Revel, G., & Barbe, J. C. (2013). Study of sensory interactions among red wine fruity esters in a model solution. *Journal of Agricultural and Food Chemistry, 61*(36), 8504-8513. doi:10.1021/jf4018405

Lyu, J. H., Ma, Y., Xu, Y., Nie, Y., & Tang, K. (2019). Characterization of the key aroma compounds in marselan wine by gas chromatography-olfactometry, quantitative measurements, aroma recombination, and omission tests. *Molecules, 24*(16), 2978.

Ma, Y., Tang, K., Xu, Y., & Li, J. M. (2017). Characterization of the key aroma compounds in Chinese Vidal icewine by gas chromatography-olfactometry, quantitative measurements, aroma recombination, and omission tests. *Journal of Agricultural and Food Chemistry, 65*(2), 394-401. doi:10.1021/acs.jafc.6b04509

Ma, Y., Tang, K., Xu, Y., & Thomas-Danguin, T. (2021). Perceptual interactions among food odors: Major influences on odor intensity evidenced with a set of 222 binary mixtures of key odorants. *Food Chemistry, 353*, 129483.

Ma, Y., Xu, Y., & Tang, K. (2021). Aroma of icewine: a review on how environmental, viticultural, and oenological factors affect the aroma of icewine. *Journal of Agricultural and Food Chemistry, 69*(25), 6943–6957.

Machiels, D., Istasse, L., & van Ruth, S. M. (2004). Gas chromatography-olfactometry analysis of beef meat originating from differently fed Belgian Blue, Limousin and Aberdeen Angus

bulls. *Food Chemistry, 86*(3), 377-383.

Niu, Y. W., Liu, Y., & Xiao, Z. B. (2020). Evaluation of perceptual interactions between ester aroma components in Langjiu by GC-MS, GC-O, sensory analysis, and vector model. *Foods, 9*(2), 183.

Niu, Y. W., Wang, P., Xiao, Z., Zhu, J., Sun, X., & Wang, R. (2019). Evaluation of the perceptual interaction among ester aroma compounds in cherry wines by GC-MS, GC-O, odor threshold and sensory analysis: an insight at the molecular level. *Food Chemistry, 275*, 143-153. doi:10.1016/j.foodchem.2018.09.102

Noble, A. C., Arnold, R. A., Buechsenstein, J., Leach, E. J., Schmidt, J. O., & Stern, P. M. (1987). Modification of a standardized system of wine aroma terminology. *American Journal of Enology and Viticulture, 38*(2), 143-146.

Polášková, P., Herszage, J., & Ebeler, S. E. (2008). Wine flavor: chemistry in a glass. *Chemical Society Reviews, 37*(11), 2478-2489.

Pollien, P., Ott, A., Montigon, F., Baumgartner, M., Muñoz-Box, R., & Chaintreau, A. (1997). Hyphenated headspace-gas chromatography-sniffing technique: screening of impact odorants and quantitative aromagram comparisons. *Journal of Agricultural and Food Chemistry, 45*(7), 2630-2637.

Ryan, J. A., Ulrich, J. M., Thielen, W., Teetor, P., Bronder, S., & Ulrich, M. J. M. (2020). Package 'quantmod'.

Sáenz-Navajas, M. P., Campo, E., Culleré, L., Fernández-Zurbano, P., Valentin, D., & Ferreira, V. (2010). Effects of the nonvolatile matrix on the aroma perception of wine. *Journal of Agricultural and Food Chemistry, 58*(9), 5574-5585.

Schieberle, P. (1995). New developments in methods for analysis of volatile flavor compounds and

their precursors. In A. G. Gaonkar (Ed.), *Characterization of Food* (pp. 403-431). Amsterdam: Elsevier.

Siebert, T. E., Barker, A., Pearson, W., Barter, S. R., Lopes, M. A. B., Darriet, P., . . . Francis, I. L. (2018). Volatile compounds related to 'stone fruit' aroma attributes in Viognier and Chardonnay wines. *Journal of Agricultural and Food Chemistry, 66*(11), 2838-2850. doi:10.1021/acs.jafc.7b05343

Tempere, S., Schaaper, M. H., Cuzange, E., De Lescar, R., De Revel, G., & Sicard, G. (2016). The olfactory masking effect of ethylphenols: characterization and elucidation of its origin. *Food Quality and Preference, 50*, 135-144. doi:10.1016/j.foodqual.2016.02.004

Thomas-Danguin, T., Rouby, C., Sicard, G., Vigouroux, M., Farget, V., Johanson, A., . . . De Graaf, C. (2003). Development of the ETOC: a European test of olfactory capabilities. *Rhinology, 41*(3), 134-151.

Thomas-Danguin, T., Sinding, C., Romagny, S., El Mountassir, F., Atanasova, B., Le Berre, E., . . . Coureaud, G. (2014). The perception of odor objects in everyday life: a review on the processing of odor mixtures. *Frontiers in Psychology, 5*, 504. doi:10.3389/fpsyg.2014.00504

Thomsen, M., Dosne, T., Beno, N., Chabanet, C., Guichard, E., & Thomas‐Danguin, T. (2017). Combination of odour–stimulation tools and surface response methodology for odour recombination studies. *Flavour and Fragrance Journal, 32*(3), 196-206. doi:10.1002/ffj.3376

Tomasino, E., Song, M., & Fuentes, C. (2020). Odor perception interactions between free monoterpene isomers and wine composition of Pinot Gris wines. *Journal of Agricultural and Food Chemistry, 68*(10), 3220-3227. doi:10.1021/acs.jafc.9b07505

Van Ruth, S. M. (2001). Methods for gas chromatography-olfactometry: a review. *Biomol. Eng.,*

703 *17*(4-5), 121-128.

704 Villiere, A., Le Roy, S., Fillonneau, C., & Prost, C. (2018). InnOscent system: advancing flavor
705 analysis using an original gas chromatographic analytical device. *J. Chromatogr. A, 1535*,
706 129-140. doi:10.1016/j.chroma.2017.12.053

707 Williams, R. C., Sartre, E., Parisot, F. A., Kurtz, A. J., & Acree, T. E. (2009). A gas
708 chromatograph-pedestal olfactometer (GC-PO) for the study of odor mixtures.
709 *Chemosensory Perception, 2*(4), 173.

710 Yu, H., Xie, T., Xie, J., Chen, C., Ai, L., & Tian, H. (2020). Aroma perceptual interactions of
711 benzaldehyde, furfural, and vanillin and their effects on the descriptor intensities of
712 Huangjiu. *Food Research International, 129*, 108808. doi:10.1016/j.foodres.2019.108808

713

714

715 **Figure captions**

716 **Figure 1** Schematic representation of the GC−O and Olfactoscan analysis, and GC × GC−TOFMS
717 analysis for Vidal icewine.

718 **Figure 2** Results of detection frequency data processing for data obtained in GC−O and Olfactoscan
719 analysis of Vidal icewine. Graphs were arranged according to analysis methods (column) and data
720 processing methods (row). For each column of graphs: GCO refers to GC−O analysis; OLFH refers
721 to Olfactoscan analysis within the aroma buffer of icewine at a high concentration; OLFL refers to
722 Olfactoscan analysis within the aroma buffer of icewine at a low concentration. The numbers refer
723 to the identity of odorants, as given in Table 2. The top graphs **(a)** illustrate the detection frequency
724 raw data for each analysis method; the middle graphs **(b)** illustrate the nasal impact frequency
725 (NIF, %) of the highest peaks for odor zones (OZs) based on average RIs, which were defined in a
726 semiautomatic method for each analysis method; and the bottom graphs **(c)** illustrate the final OZs
727 based on average RIs after manual checking. Only OZs with NIF ≥ 20% (4/19) were considered in
728 the final OZ data, and the OZs with NIF ≥ 60% (12/19) were marked as high impact (in purple
729 color); otherwise, they were marked as normal impact (in light blue).

730 **Figure 3** Nasal impact frequency (NIF, %) comparisons between GC−O and Olfactoscan analysis
731 of Vidal icewine. An NIF difference above 20% (4/19) was considered a threshold for a significant
732 mixture-induced effect for a peak. The numbers refer to the identity of odorants, as given in Table 2.
733 **(a)** The NIF difference between GC−O analysis and Olfactoscan analysis within the aroma buffer of
734 icewine at a high concentration. If the NIF for OLFH was significantly lower than the NIF for GCO,
735 a masking effect (in purple color) occurred; if the NIF for OLFH was significantly higher than the
736 NIF for GCO, enhancement effect (in light blue color) occurred. **(b)** The NIF difference between
737 GC−O analysis and Olfactoscan analysis within the aroma buffer of icewine at a low concentration.

738 The NIF difference between GC–O analysis and Olfactoscan analysis at both high and low
739 concentrations. **(c)** The peak of GC–O analysis and the effect occurring within the aroma buffer of
740 icewine for each peak are marked. The effects including masking occurring at both concentrations
741 (in red); enhancement occurring at both concentrations (in dark blue); masking occurring at high
742 concentration (in purple); enhancement occurring at high concentration (in light blue); masking
743 occurring at low concentration (in pink); enhancement occurring at low concentration (in light
744 green); and no significant effect occurring at either concentration (in black). **(d)** Peak of Olfactoscan
745 analysis within the aroma buffer of icewine at high (deep orange) and low (light orange)
746 concentrations. E.g.: For the NIF of peak 11, the aroma buffer of icewine at high level was marked
747 in deep orange and the aroma buffer of icewine at low level was marked in light orange, the NIF at
748 low level (47.4%) is higher than the NIF at high level (21.1%).
749 **Figure 4** Principal component analysis (PCA) biplot of Vidal icewine showing the descriptor
750 trajectories of highly impacted odor peaks (NIF> 60%) over icewine background odor levels: zero
751 level (GCO), low level (OLFL) and high level (OLFH). The beginning of the trajectory was GCO
752 data (position at the peak number), the end of the trajectory was OLFH data (position at the solid
753 dots), and the turning point was OLFL data. The numbers refer to the identity of odorants, as given
754 in Table 2. **(a)** The first 2 dimensions of the PCA map of odor descriptors. **(b)** The 3rd and 4th
755 dimensions of the PCA map of odor descriptors.

Table 1 Odor Zones (OZs) of Vidal Icewine determined in GC−O and Olfactoscan Analysis by Detection Frequency (DF) Method. NIF (%) corresponded to the proportion of detection for each OZ.

OZ	Retention indices (RI)			NIF (%), n=19			Odor descriptor		
number	Average	Start	End	GCO	OLFH	OLFL	GCO	OLFH	OLFL
1	980	970	990	73.7	15.8	15.8	strawberry, strawberry, fruity, potato	honey	change
2	1008	1000	1015	52.6	36.8	42.1	plastic, solvent	increase, rubber	new odor, nut, plastic
3	1020	1015	1025	42.1	10.5	15.8	flowery, pineapple	change	cassis
4	1048	1040	1055	63.2	26.3	15.8	fruity, plastic, solvent	change	fruity
5	1068	1060	1075	52.6	26.3	42.1	strawberry	fruity increase	prune, strawberry
6	1088	1080	1095	57.9	15.8	21.1	cabbage, caramel, fruity, orange, solvent	change	change
7	1115	1105	1125	57.9	63.2	52.6	plastic, nut	alcohol, apple, fruity, plastic	nut, plastic

8	1135	1130	1140	31.6	26.3	31.6	banana, cabbage	metallic	change
9	1153	1145	1160	36.8	36.8	26.3	flowery, fruity	flowery, fruity increase	change
10	1170	1160	1180	36.8	47.4	42.1	banana, caramel, chocolate, fruity, strawberry	flowery, fruity increase, red wine, sour	change
11	1193	1185	1200	36.8	21.1	47.4	baked, baked vanilla	change	caramel increase, sweet
12	1215	1200	1230	100.0	68.4	68.4	cheese, flowery, caramel, chocolate, sour	ethanol, fruity increase, increase, strawberry jam	flowery, increase
13	1235	1230	1240	15.8	15.8	42.1	fruity	change	change
14	1255	1245	1265	57.9	31.6	42.1	fruity, strawberry	fruity increase	flowery increase
15	1283	1275	1290	26.3	31.6	47.4	caramel	alcohol	flowery increase
16	1305	1300	1310	21.1	26.3	26.3	apple peel, fruity	flowery	nut
17	1318	1310	1325	63.2	68.4	68.4	mushroom	mushroom, potato	mushroom, fruity
18	1335	1325	1345	89.5	89.5	63.2	baked cocoa, bread, fruity, nut, roasted nut, sour	curry, fruity, meaty soup, nut roasted	mushroom, new odor, nut, plastic

19	1355	1345	1365	47.4	63.2	52.6	baked	pine	change
20	1373	1365	1380	47.4	31.6	36.8	flowery, menthol	cheese, tablet	fruity, rose
21	1400	1390	1410	57.9	57.9	63.2	cake, grass, herb	alcohol, passion fruit, plastic, strawberry	grass
22	1415	1410	1420	31.6	10.5	31.6	fruity	change	rose
23	1425	1420	1430	47.4	57.9	47.4	mushroom	flowery, fruity, mushroom, plastic	cabbage, nut
24	1438	1430	1445	26.3	36.8	42.1	solvent	fruity change, increase	change
25	1453	1445	1460	63.2	57.9	63.2	baked, coffee, coffee	flowery, nut increase, roasted hazelnuts, toast	fruity, nut
26	1465	1460	1470	21.1	36.8	47.4	unknown	malty, plastic, roasted	fruity, new odor, nut
27	1478	1470	1485	68.4	89.5	89.5	potato, cooked potato, soy sauce	potato, cooked potato	animal food, cooked potato, potato
28	1490	1485	1495	57.9	47.4	63.2	animal, curry, sweet	pine	fruity, mint candy,

									plastic, potato
29	1503	1495	1510	47.4	36.8	52.6	plastic, coffee, fruity, pine	grapefruit, plastic	acid, another plastic, potato
30	1518	1510	1525	31.6	15.8	31.6	unknown	sweet	fruity, soy sauce
31	1533	1525	1540	26.3	36.8	36.8	unknown	animal, soy sauce	bad soy sauce
32	1565	1555	1575	47.4	52.6	36.8	flowery, fruity with something	fruity, soy sauce increase	hay, increase
33	1583	1575	1590	36.8	31.6	42.1	caramel, fruity, vanilla	fruity change	change
34	1600	1590	1610	57.9	47.4	63.2	flowery, animal, mint candy	nut change, peach, red wine	mint candy
35	1628	1615	1640	52.6	21.1	26.3	bread, cereal, sugar, sweet	change	change
36	1650	1640	1659	78.9	94.7	89.5	cheese, hay, solvent	cheese, hay	bad odor, flowery, hay
37	1665	1660	1670	57.9	26.3	52.6	almond, baked cocoa, caramel	animal, smoky	cheese, new odor

38	1668	1670	1685	31.6	52.6	42.1	herb, solvent acid	flowery, fruity	rose
39	1705	1685	1720	94.7	100.0	100.0	cheese, acid, bad odor	cheese, sweaty, unpleasant	cheese, new odor, strong sweaty
40	1738	1725	1750	31.6	26.3	36.8	nut	change	nut
41	1758	1750	1765	42.1	42.1	31.6	cereal, cheese, nut	honey increase	caramel increase
42	1773	1765	1780	42.1	21.1	47.4	alcohol, red fruit, sweet	change	mint, new odor
43	1785	1780	1790	26.3	15.8	42.1	unknown	change	honey caramel
44	1833	1825	1840	10.5	26.3	36.8	roasted	increase	caramel change
45	1853	1845	1860	26.3	31.6	42.1	unknown	citrus, metallic	honey increase, vegetable
46	1870	1860	1880	68.4	57.9	36.8	fruity, fruity jam, honey	animal	mint cold, new odor, sweet
47	1885	1880	1890	47.4	52.6	31.6	baked, fruity alcohol, fruity, honey	sweet	mint cold increase

48	1903	1890	1915	63.2	68.4	89.5	flowery, smoky, solvent, wine, wood	flowery, sweet	honey, plastic, smoky, sweet
49	1945	1935	1955	52.6	63.2	42.1	fruity, plastic, rose, sweet, wine	flowery, sweet	sweet
50	1963	1955	1970	52.6	42.1	36.8	alcohol, rose	sweet, wine	prune
51	1990	1980	2000	36.8	26.3	26.3	honey, fruity alcohol	increase	change
52	2023	2010	2030	31.6	52.6	31.6	honey	apple, grapefruit, honey, increase, sweet increase	fruity
53	2050	2040	2060	52.6	26.3	36.8	alcohol, fruity alcohol, fruity, honey with something	apple, apricot	smoky
54	2088	2080	2095	47.4	26.3	36.8	alcohol, fruity alcohol, red fruit, vegetable	apricot	honey increase
55	2108	2095	2120	52.6	47.4	31.6	apricot, bread	apricot, fruity, red	change

56	2133	2120	2145	47.4	57.9	42.1	fruity, vegetable	apricot, mushroom, rotten, sugar	flowery, sweet increase
57	2153	2145	2160	26.3	31.6	21.1	caramel milk tea, jam	candy, pineapple	sweet increase
58	2170	2160	2185	47.4	57.9	52.6	baked, bread, caramel milk tea, honey	jam	apricot, fruity, sweet
59	2193	2185	2205	63.2	31.6	42.1	candy, caramel milk tea, caramel, cereal, jam	caramel, fruity candy, peach, sugar	apricot
60	2220	2210	2230	52.6	42.1	42.1	caramel, caramel baked, peach candy, sugar	increase, peach increase, strawberry	soy sauce, sweet
61	2243	2230	2255	57.9	42.1	47.4	baked caramel, cake, caramel	red fruit, strawberry	fruity candy
62	2270	2260	2280	47.4	47.4	52.6	cake	increase, peach increase, smoky, strawberry	caramel increase, fruity
63	2288	2280	2295	47.4	15.8	26.3	baked caramel, bread	peach	flowery, red fruit

64	2308	2295	2320	47.4	26.3	47.4	caramel, fruity	increase	caramel, fruity
65	2333	2320	2345	47.4	47.4	57.9	caramel, fruity, vegetable, fruity baked	increase	mango, new odor
66	2353	2345	2360	10.5	52.6	10.5	fruity	increase, peach, strawberry	change
67	2370	2360	2380	52.6	15.8	47.4	alcohol, baked sauce, fruity	fruity	new odor, papaya, smoky
68	2400	2390	2410	57.9	31.6	57.9	caramel, caramel baked, sugar wine	increase	fruity candy increase
69	2450	2440	2460	52.6	36.8	42.1	baked, spicy, sugar wine	increase, nut	prune

Odor Zones listed in the table were ranked by their appearances from 1 to 69, and each OZ was featured by 1) the first, the last and the average RI of the response given by all subjects; 2) [a] Nasal Impact Frequency (NIF, %), which corresponded to the proportion of detection by the panelists of each OZ.; 3) Odor descriptors given by subjects, the odor descriptor was ordered by frequency from high to low. The descriptor 'change' was used by the panelists when they qualified an OZ related to a modification (i.e. a 'change') of the background odor, but they did not provide additional descriptors to qualify the 'change'.

764 Table 2 Identification of Odor Zones (OZs) in Vidal Icewine by GC–O–, GC−MS and GC × GC−TOFMS

OZ number	Retention indices (RI) GCO [a]	TofMS [b]	NIST [c]	Compounds[d]	Odor descriptors [e]	Identification [f]	CAS.	Quantitative mass
1	980	961	955	ethyl isobutyrate	sweet, ethereal, fruity, alcoholic, fusel, rummy	MS;RI;O;S	97-62-1	71
2	1008	977	970	2,3-butanedione*	butter, sweet, creamy, pungent, caramel	MS;RI;O;S	431-03-8	86
3	1020	1025	1015	isobutyl acetate	sweet, fruity, ethereal, banana, tropical	MS;RI;O;S	110-19-0	43
4	1048	1044	1028	ethyl butyrate	fruity, juicy, pineapple, cognac	MS;RI;O;S	105-54-4	71
5	1068	1062	1050	ethyl 2-methylbutyrate	sharp, sweet, green, apple, fruity	MS;RI;O;S	7452-79-1	102
6	1088	1067	1060	ethyl isovalerate	fruity, sweet, apple,	MS;RI;O;S	108-64-5	88

					pineapple			
7	1115	1088	1099	2-methyl-1-propanol	ethereal, winey, cortex	MS;TOFMS;RI;O;S	78-83-1	42
8	1135	1127	1117	isoamyl acetate	sweet, fruity, banana, solvent	MS;TOFMS;RI;O;S	123-92-2	70
9	1153	1140	1133	ethyl valerate	sweet, fruity, apple, pineapple, green, tropical	MS;TOFMS;RI;O;S	539-82-2	88
10	1170	1181	1176	pentyl acetate	ethereal, fruity, banana, pear, banana, apple	TOFMS;RI;O	628-63-7	61
11	1193	1196	1183	2-heptanone	fruity, spicy, sweet, herbal, coconut, woody	TOFMS;RI;O	110-43-0	58
12	1215	1209	1205	3-methyl-1-butanol	fuel oil, alcoholic, whiskey, fruity, banana	MS;TOFMS;RI;O;S	123-51-3	39
13	1235	1220	1216	2-hexanol	chemical, winey, fruity, fatty, terpene, cauliflower	TOFMS;RI	626-93-7	45

13	1235	1237	1235	2-pentylfuran	fruity, green, earthy, beany, vegetable, metallic	TOFMS;RI	3777-69-3	81
14	1255	1239	1220	ethyl hexanoate	sweet, fruity, pineapple, waxy, green, banana	MS;TOFMS;RI;O;S	123-66-0	88
15	1283	1280	1267	ethyl pyruvate	ether, fruity, sweet, sharp, rum, vegetable, caramel	TOFMS;RI;O	617-35-6	43
16	1305	1297	1285	2-octanone	earthy, weedy, natural, woody, herbal	TOFMS;RI	111-13-7	58
17	1318	1314	1313	1-octen-3-one	herbal, mushroom, earthy, musty, dirty	TOFMS;RI;O;S	4312-99-6	70
18	1335		1331	2-acetyl-1-pyrroline	popcorn, toasted, grain, malty	RI;O	85213-22-5	

19	1355	1351	1360	1-hexanol	ethereal, fuel oil, fruity, alcoholic, sweet, green	MS;TOFMS;RI;O;S	111-27-3	43
20	1373	1363	1358	*cis*-rose oxide	green, red rose, spicy, fresh, geranium	MS;TOFMS;RI;O;S	16409-43-1	139
21	1400	1384	1386	(*Z*)-3-hexen-1-ol	fresh, green, cut grass, foliage, vegetable, herbal, oily	MS;TOFMS;RI;O;S	928-96-1	67
22	1415	1439	1436	ethyl octanoate	fruity, wine, waxy, sweet, apricot, banana, brandy, pear	MS;TOFMS;RI;O;S	106-32-1	88
23	1425	1447	1447	1-octen-3-ol*	mushroom, earthy, green, oily, fungal, raw chicken	MS;TOFMS;RI;O;S	3391-86-4	57
24	1438	1448	1451	linalyl oxide	earthy, floral, sweet, woody	MS;TOFMS;RI;O	5989-33-3	59

25	1453		1449	2-ethyl-3,5-dimethyl pyrazine	burnt almonds, roasted nuts, coffee	RI;O	13925-07-0	
26	1465	1453	1460	1-heptanol	musty, leafy, violet, herbal, green, sweet, woody, peony	MS;TOFMS;RI;S	111-70-6	70
27	1478	1476	1458	methional	musty, potato, tomato, earthy, vegetable, creamy	TOFMS;RI;O;S	3268-49-3	47
28	1490	1480	1479	nerol oxide	green, weedy, cortex, herbal, diphenyl, oxide, narcissus, celery	MS;TOFMS;RI;O	1786-08-9	68
29	1503	1489	1484	2-ethyl-1-hexanol	citrus, fresh, floral, oily, sweet	MS;TOFMS;RI;O	104-76-7	57
30	1518	1523	1524	ethyl 3-hydroxybutyrate	fruity, green, grape, tropical, apple skin	MS;TOFMS;RI	5405-41-4	88

				ethyl				
31	1533	1544	1545	2-hydroxy-4-methyl valerate	fresh blackberry	TOFMS;RI	10348-47-7	87
32	1565	1553	1537	*β*-linalool	citrus, floral, sweet, bois de rose, woody, green, blueberry	MS;TOFMS;RI;O;S	78-70-6	71
33	1583		1561	ethyl 3-methylthiopropionate	sulfur, metallic, pineapple, fruity, ripe pulpy tomato	RI;O	13327-56-5	
34	1600	1613	1620	hotrienol	sweet, tropical, fennel, ginger	MS;TOFMS;RI;O	29957-43-5	71
35	1628	1662	1648	benzeneacetaldehyde	green, sweet, floral, hyacinth, clover, honey, cocoa	TOFMS;RI;O	122-78-1	91

36	1650	1670	1662	2-methylbutanoic acid	pungent, acid, cheese	MS;TOFMS;RI;O;S	116-53-0	74
36	1650	1673	1680	acetophenone	sweet, pungent, hawthorn, mimosa, almond, acacia, chemical	TOFMS;RI;O	98-86-2	105
37	1665		1660	2-acetylthiazole	earthy	RI;O	932-16-1	
38	1668	1679	1687	diethyl succinate	mild, fruity, cooked apple	TOFMS;RI;O;S	123-25-1	101
39	1705		1665	3-methylbutanoic acid*	sour, stinky, feet, sweaty, cheese, tropical	MS;RI;O;S	503-74-2	
40	1738	1724	1738	3-(methylthio)-1-propanol	sulfurous, onion, sweet, soup, vegetable	TOFMS;RI;O;S	505-10-2	106
41	1758	1741	1732	linalool oxide (*trans*-pyranoid)	woody	MS;TOFMS;RI;O	39028-58-5	68
42	1773	1797	1779	ethyl phenylacetate*	sweet, floral, honey, rose,	MS;TOFMS;RI;O;S	101-97-3	91

					balsam, cocoa			
43	1785	1798	1794	1-(4-methylphenyl)ethanone	hawthorn, sweet, mimosa, cherry	TOFMS;RI	122-00-9	119
44	1833	1823	1817	γ-heptalactone	sweet, coconut, nutty, caramel, hay	MS;TOFMS;RI;O	105-21-5	85
45	1853	1827	1829	phenethyl acetate*	floral, rose, sweet, honey, fruity, tropical	MS;TOFMS;RI;S	103-45-7	104
46	1870	1832	1840	β-damascenone*	natural sweet, fruity, rose, plum, grape, raspberry, sugar	MS;TOFMS;RI;O;S	23696-85-7	69
46	1870	1845	1853	3-mercapto-1-hexanol	sulfurous, fruity, tropical	TOFMS;RI;O;S	51755-83-0	100
46	1870	1848	1840	geraniol*	sweet, floral, fruity, rose, waxy, citrus	MS;TOFMS;RI;O;S	106-24-1	69

47	1885	1854	1857	*p*-cymen-8-ol	sweet, fruity, cherry, floral, camphor	MS;TOFMS;RI;O	1197-01-9	135
48	1903	1871	1859	guaiacol*	phenolic, smoke, spice, vanilla, woody	MS;TOFMS;RI;O;S	90-05-1	109
49	1945	1918	1925	phenylethyl alcohol*	floral, rose, dried rose, flower, rose water	MS;TOFMS;RI;O;S	60-12-8	92
50	1963	1936	1923	*γ*-octalactone	sweet, coconut, waxy, creamy, dairy, fatty	MS;TOFMS;RI;O	104-50-7	85
51	1990	1988	1988	*δ*-octalactone	sweet, fatty, coconut, tropical, dairy	MS;TOFMS;RI;O	698-76-0	99
52	2023	2013	2008	phenol	phenolic, plastic, rubber	MS;TOFMS;RI;O	108-95-2	94
53	2050	2047	2042	*γ*-nonalactone	coconut, creamy, waxy, sweet, buttery, oily	MS;TOFMS;RI;O	104-61-0	85
54	2088	2066	2056	4-hydroxy-2,5-dimet	sweet, cotton candy,	TOFMS;RI;O;S	3658-77-3	85

				hyl-3(2*H*)-furanone (furaneol)*	caramel, strawberry, sugar			
55	2108		2031	4-ethylguaiacol	spicy, smoky, bacon, phenolic, clove	MS;RI;S	2785-89-9	
56	2133	2146	2127	ethyl cinnamate	sweet, balsam, fruity, spicy, powdery, berry, plum	MS;TOFMS;RI;O;S	103-36-6	131
57	2153	2091	2088	4-hydroxy-5-ethyl-2-methyl-3(2*H*)-furanone (homofuraneol)	sweet, caramel, bready, maple, brown sugar, burnt	MS;TOFMS;RI;O;S	27538-09-6	43
58	2170	2161	2144	*γ*-decalactone	fresh, oily, waxy, peach, coconut, buttery, sweet	MS;TOFMS;RI;O;S	706-14-9	85
59	2193	2178	2167	eugenol	sweet, spicy, clove, woody	MS;TOFMS;RI;O;S	97-53-0	164

60	2220	2208	2203	4-vinylguaiacol	dry, woody, fresh, amber, cedar, roasted, peanut	MS;TOFMS;RI;O;S	7786-61-0	135
61	2243	2213	2208	*δ*-decalactone	fresh, sweet, oily, coconut, fruity, peach, creamy, dairy	MS;TOFMS;RI;O	705-86-2	99
62	2270	2216		thymol	herbal, thyme, phenolic, medicinal, camphor	TOFMS;RI;O	89-83-8	115
63	2288	2276	2270	*γ*-undecalactone	fruity, peach, creamy, fatty, apricot, coconut	TOFMS;RI;O	104-67-6	85
64	2308	2281	2296	syringol	smoky, phenolic, balsamic, bacon, powdery, woody	TOFMS;RI;O	91-10-1	154
65	2333	2319	2311	4-methyl-5-thiazolee thanol	fatty, cooked beef juice	TOFMS;RI	137-00-8	112

66	2353	2333	2336	9-decenoic acid	waxy, green, fruity, fatty, soapy	TOFMS;RI	14436-32-9	69
66	2353	2340	2347	geranic acid	dry, weedy, acidic, green, moldy, feet, woody	TOFMS;RI	459-80-3	100
66	2353	2359	2327	isophytol	mild, floral, herbal, green	TOFMS;RI	505-32-8	71
67	2370	2363	2350	isoeugenol	sweet, spicy, clove, woody, carnation, floral	MS;TOFMS;RI;O	97-54-1	164
68	2400	2415	2415	*γ*-dodecalactone	fatty, peach, sweet, metallic, fruity	MS;TOFMS;RI;O	2305-05-7	85
69	2450	2447	2445	*δ*-dodecalactone	fresh sweet metallic peach oily coconut buttery	TOFMS;RI	713-95-1	99

765 [a] RI calculated from GC−O and Olfactoscan analysis; [b] RI calculated from GC × GC−TOFMS analysis; [c] RI reported in NIST library on similar column;

766 [d] Compounds tagged with an '*' were found to have different RI calculated from the GCO analysis and from the GC × GC−TOFMS analysis; the

767 identification of these odor zones have been verified by injecting pure standards; [e] descriptors obtained from the database of The Good Scents Company

768 (http://www.thegoodscentscompany.com/); [f] Peak identified by: 1) GC × GC−TOFMS analysis (TOFMS), the first six odorants were not identified by

769 TOFMS due to the setting of solvent delay; 2) GC–MS (MS) and comparing the RI and odor descriptor of a candidate compound with the RI and odor

770 descriptor of its pure standard under the same GC conditions as in GC–O (S); 3) comparing the odor descriptor of a candidate compound with its odor

771 descriptor reported in the database (O); and 4) comparing the experimental RI of a candidate compound with the RI reported in the NIST Mass Spectral

772 Library (RI).

773 Figure 1

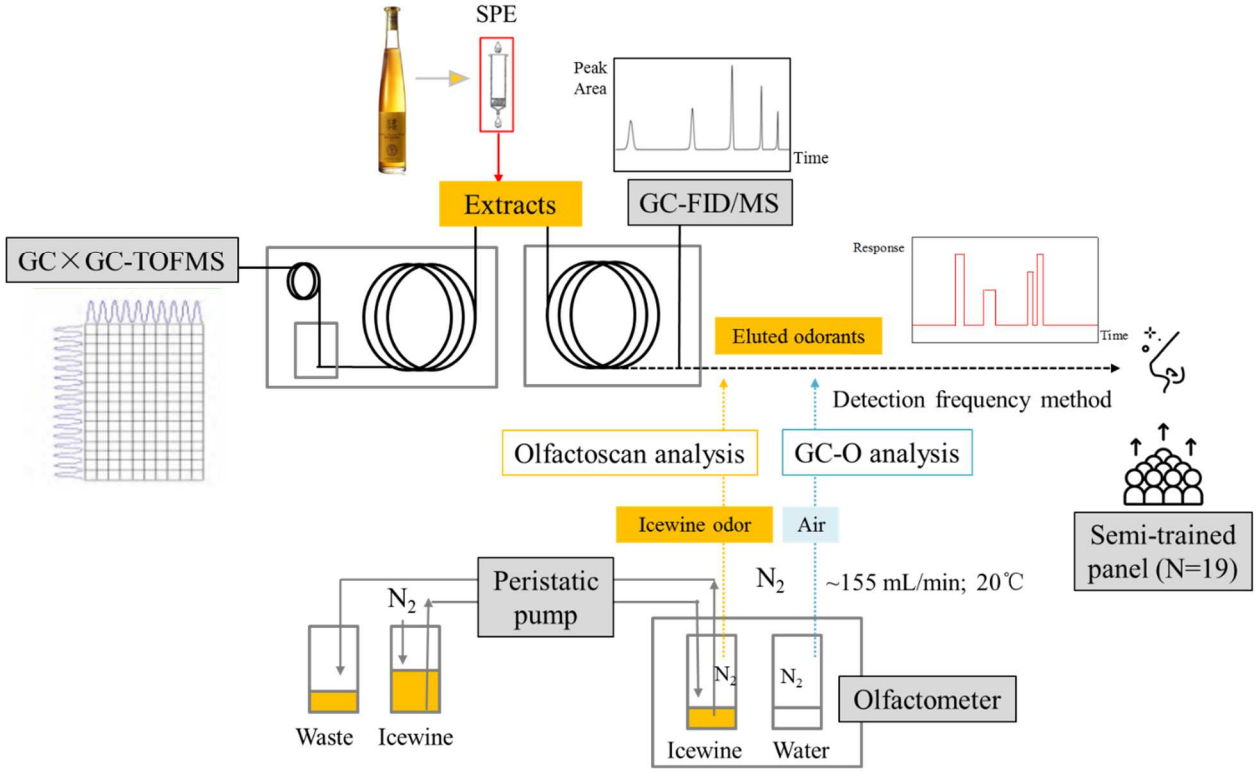

774

775

776 Figure 2

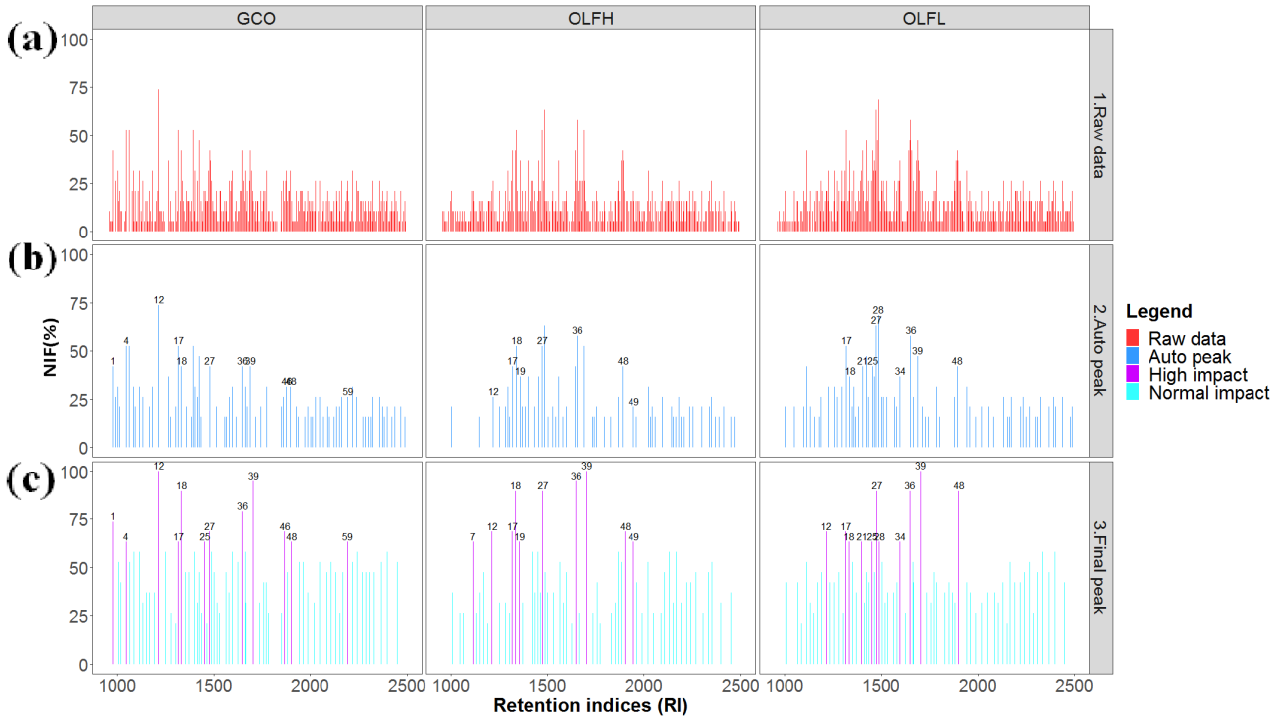

777

778

779 Figure 3

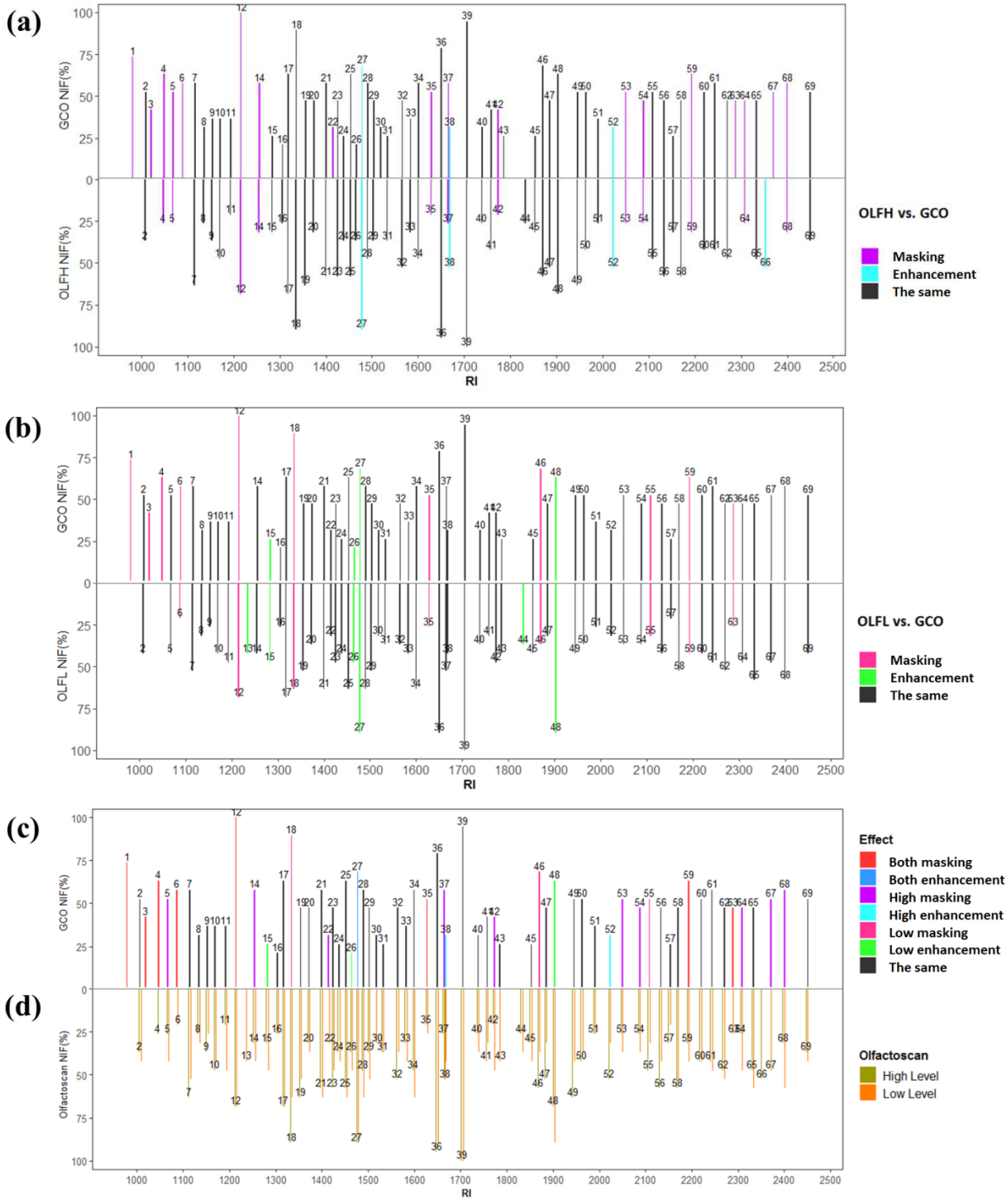

780

781

782 Figure 4

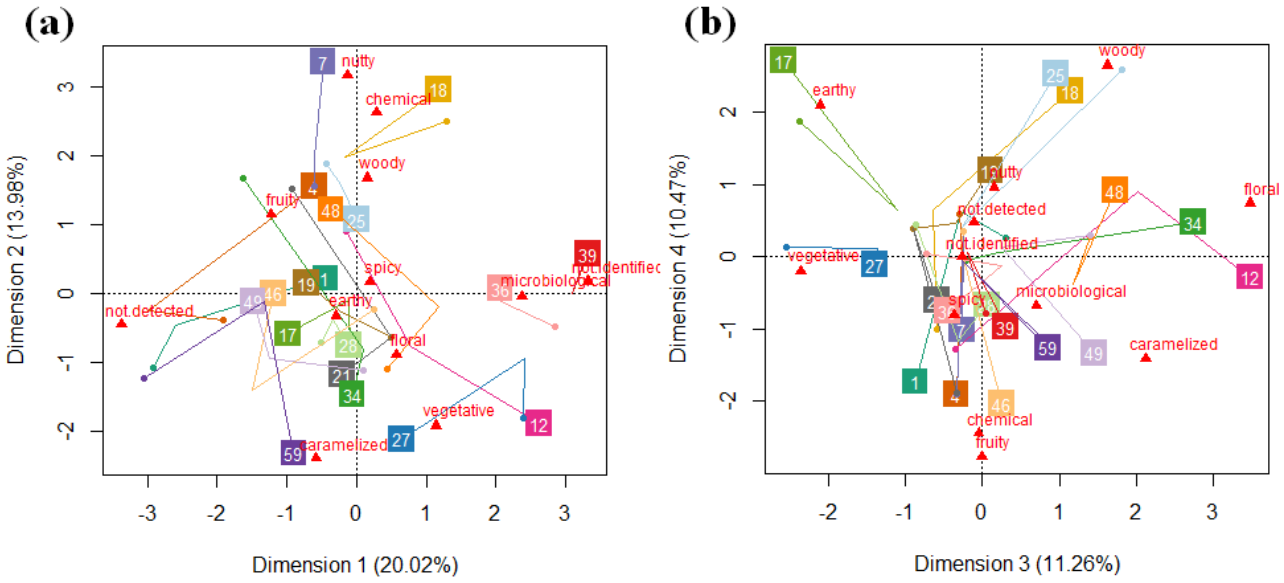

783